UNIVERSITÉ DE PAU ET DES PAYS DE L'ADOUR
UNIVERSIDAD DE OVIEDO

MASTER'S PROJECT

Optimization of chromium (VI) free deanodizing process for aluminium alloy 2024-T3

Víctor García Montoto

People in charge of the project:

Jérôme Frayret

Jean-Charles Dupin

18/07/2016

Universidad de Oviedo

UNIVERSITÉ DE PAU ET DES PAYS DE L'ADOUR

IPREM
Institut des sciences analytiques et de physico-chimie pour l'environnement et les matériaux

Summary.

1. Introduction.

1.1. Brief introduction about aluminium.

Aluminium is the most abundant metal and the third most abundant element in the Earth's crust (8.30% abundant) after Oxygen and Silicon. It is a chemical element situated in the boron group of the Periodic Table (group 13th) with symbol Al and atomic number 13. Naturally it is found combined in over 270 different minerals, mostly as Al_2O_3 (corindon), or in a hydroxide form in some silicates or bauxites [1].

Aluminium is a silvery-white metal with many valuable properties such as low toxicity and higher electrical conductivity. Because of its low density and its ability to resist corrosion through the phenomenon of passivation it is mostly used as a metallic material or in alloys specially in the aerospace industry. Another property of Aluminium is its chemical reactivity. It is a widely used and a very good reducing agent.

Aluminium metal is obtained by electrolytic reduction of a mixture which contains alumina (around 10%), 3NaF/AlF3 (artificial cryolyte, around 80%) and CaF2 (5-7%) [1]. With this composition it is optimised the melting point and also the medium conductivity. Temperature during this process is around 1000 °C. The electrolyte is placed in an iron vat lined with graphite. This vat works as the cathode and the anodes made of pure carbon are inserted into the electrolyte from the top (Södeberg electrodes).

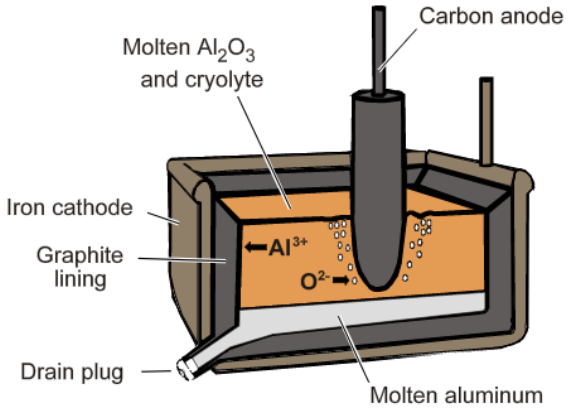

Figure 1. Diagram of the typical set up of electrolytic obtaining of Aluminium [2].

Pure aluminium naturally forms a thin surface layer of aluminium oxide on contact with the oxygen present in the atmosphere. This layer creates a physical barrier against corrosion in many environments. This protective coating is frequently enhanced by the process of anodization, process that will be studied later [2].

This report is focused on the Aluminium alloy 2024-T3, which has been widely used in aerospace applications because of its superior mechanical properties such as excellent highness, strength-to-weight radio and good fatigue properties. Nevertheless, Aluminium 2024-T3 and similar alloys have a high susceptibility to be corroded under atmospheric corrosion, specially in industrial and seacoast atmospheres, so, these alloys have to be protected against atmospheric corrosion to be useful in industry. This protection deals with the formation of a Al_2O_3 layer with excellent properties in protecting the underlying metal [3]. The chemical composition of this alloy is detailed in Table 1.

Table 1: Chemical composition (wt.%) of Aluminium Alloy 2024-T3 [3]

Al	**Cr**	**Cu**	**Fe**	**Mg**	**Mn**	**Others**	**Si**	**Ti**	**Zn**
90.7-	Max.	3.8-4.9	Max.	1.2-1.8	0.3-0.9	Max.	Max.	Max.	Max.
94.7	0,1		0.5			0.15	0.5	0.15	0.25

To protect aluminium alloys against corrosion, the most known method and the one which is going to be studied in this work is the anodizing process. Nevertheless, it should be also pointed out another process, usually carried out after anodizing, which gives a better protection against corrosion. It is the sealing process.

1.2. Anodizing process of aluminium alloys.

Anodic oxidation (anodizing) of aluminium is a technique which has been known for many years and it has many industrial applications. Although the result of anodization depends on the type of electrolyte, porous oxidation has been observed exclusively on aluminium [4].

The experimental set-up for anodizing comprises the classical components in electrolysis: a reference electrode, a counterelectrode of carbon, platinum or another metal, and the working electrode which is the sample to be anodized. During the anodizing process which takes place

in an acid aqueous medium and under a fixed potential, it is possible to observe a gas liberation in the cathode surface. This is the result of the oxidation of the aluminium (the target piece and anode) [5] and the reduction of the aqueous medium to gas hydrogen. The acidity of the medium is necessary because it helps to dissolve the aluminium oxide and leads the nachbal1formation of a coating with nanopores. Reactions during anodizing process and a figure explaining the the experimental set-up are the next ones:

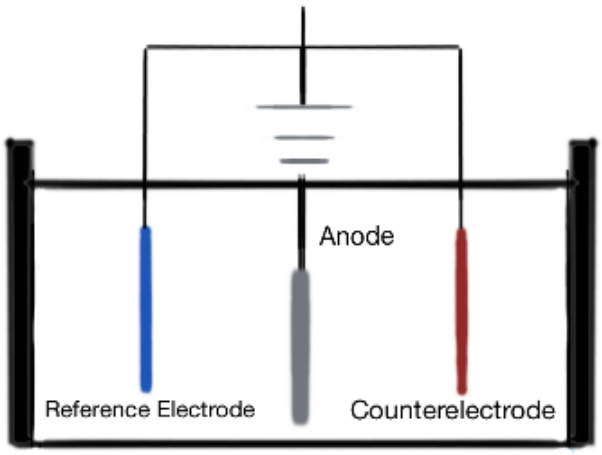

Figure 2. Graphic set up for anodizing aluminium.

$$2\,Al + 3\,H_2O \rightarrow Al_2O_3 + 6\,H^+_{(aq)} + \frac{3}{2}O_{2\,(g)} + 6\,e^- \quad \text{(Anode)} \quad (1)$$

$$2\,H_2O + 2\,e^- \rightarrow 2\,OH^-_{(aq)} + H_{2\,(g)} \quad \text{(Cathode)} \quad (2)$$

The process begins with the application of a direct current through an electrolytic solution with the aluminium alloy serving as the anode. This current releases hydrogen at the cathode as a consequence of the medium reduction and as a consequence of the redox process it is created a build-up of aluminium oxide in the surface of the alloy [5].

1.3. Formation mechanism of the anodic layer.

A brief explanation of the mechanism of this process is given by Heber [4]. In the case of aluminium, after the anodizing process a porous layer of Al_2O_3 is formed. These pores could be formed due to the establishment of a horizontal equilibrium between the surface being anodised and the aqueous medium. This equilibrium leads the formation of a colloidal $Al(OH)_3$. These colloids favour the formation of porous in the layer due to dipole forces between molecules of the hydroxide, absorbed water or electrolyte and the reduction of the surface tension of the liquid. Thus, porous formation is a consequence of the increasing inner pressure and vertically against the electrolyte. This pores allow the electrolyte solution and current to reach the aluminium substrate. However, they can also permit air or water reach the substrate and initiate corrosion, so, as a consequence, corrosion inhibitors can be used in this process.

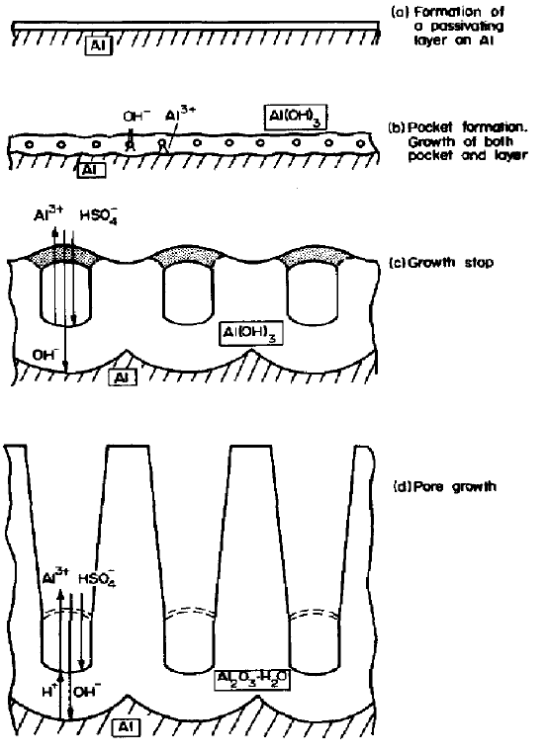

Figure 3. Formation of pores during anodizing [4].

1.4. Anodizing types.

Nowadays, several types of anodizing specifications and types are being used in aerospace industry. In this work, only two types of aluminium anodizing process applied to aeronautic applications are going to be explained and studied [5]:

- Chromic acid anodizing.
- Sulfuric acid anodizing.

1.4.1. Sulfuric Acid Anodizing (OAS).

Patented for the first time in England in 1927, Sulfuric Acid Anodizing (OAS) is the most widely used solution to produce anodized coating. The low cost of the electrolyte, sulfuric acid, the wide range of use of the process and the easy control of the parameters during the process are some of the reasons of its wide use. Depending on the required function of the anodized alloy, Sulfuric Acid Anodizing can be used to give either decorative and optical properties or protection to the aluminium alloys. In the 2000 series alloys, Sulfuric Acid Anodizing is used as a protection against corrosion.

Table 2. Conditions of sulfuric acid anodizing.

Sulfuric Acid Anodizing Parameters
• **Sulfuric Acid concentration: 180 – 200 g/L.** • **Temperature range: 18 – 21 °C.** • **Current density: < 1.5 A/dm^2.** • **Homogeneity: Constant stirring.**

With this type of anodic oxidation it is possible to obtain a 15 – 20 μm thick oxide layer, significant factor against corrosion [5].

1.4.2. Chromic Acid Anodizing (OAC).

Chromic acid was one of the first electrolytes used in the anodization techniques. The Bengough-Stuart process stablished in 1923 is the oldest one. This anodization process has been developed at the same time as the Sulfuric Acid Anodizing, but the result of this one is quite different. It is possible to obtain thinner oxide layers, with less impact on the mechanical characteristics of the pieces and with a higher friction coefficient.

Table 3. Conditions of chromic acid anodizing.

Chromic Acid Anodizing Parameters
• **Chromic Anhydride (CrO_3) concentration: 30 – 50 g/L.** • **Temperature range: 40 – 50 °C.** • **Voltage applied: 40 – 50 V during 40 min approximately.** • **Homogeneity: Constant stirring.**

With this anodization process it is possible to obtain a 2 – 7 μm thick oxide layer, quite lower than the values obtained with the OAS process [5].

The presence of Cr (VI) in the bath does not prevent chromic anodizing to still be widely used in the aeronautic industry. Coatings offering the best protection against corrosion are made with hexavalent chromium solutions despite the health concern of these compounds. Nevertheless, the use of hexavalent chromium is being restricted by the legislation [6,7] and new alternatives have been developed in order to replace it with a similar protection effect for the substrate such as the Phosphoric Oxidative Anodization or the one before mentioned, Sulfuric Acid Anodization.

1.4.3. Sealing of anodized aluminium.

Although aluminium oxide layers obtained with anodization offer a good protection against corrosion, it can be improved through the sealing process.

As it has been explained before, with the anodization process it is obtained a hexagonal columnar cell structure with one pore located at the centre of the hexagonal cell layer. Unfortunately, these pores could give some problems to the performance of the anodized oxide layer, such as not good protection against corrosion. Therefore, some post treatments after anodizing could be carried out in order to seal the pores to improve the corrosion resistance. One of the most known methods is the sealing process [8].

Sealing process is a post treatment of anodizing of aluminium which fills the pores of the aluminium oxide layer, achieving a better corrosion resistance. In the industrial field, several methods are used in order to obtain this extra protection in the alloy. Pieces studied in this work have had a sealing treatment with trivalent chromium (Cr_2O_3) after the anodizing process.

1.5. Deanodizing.

After being used for a long time, some anodized material in aeronautical industry such as helicopter pieces, plane pieces, etc. begin to suffer a lack of protection against corrosion. Thus, these pieces require a refurbishment process in which the protection has to be optimal again. In this process, pieces which need a re-anodizing process are disassembled and afterwards deanodized in order to remove completely the aluminium oxide layer before being anodized again.

1.5.1. Current Deanodization process.

The treatment employed to carry out the deanodizing process consists on a bain-marie heated acid bath which contains phosphoric acid (H_3PO_4) and chromium oxide (VI) (CrO_3), which in an aqueous is present with the form of chromic acid (H_2CrO_4) [9, 10]. The most important characteristic of this solution is that the oxide layer is removed while the underlying metal is kept intact [5].

Reactions taking place in the reaction medium are the next ones:

$$Al_2O_3 + \ 6\ \mathrm{H}^+_{(aq)} \rightarrow 2\ Al^{3+}_{(aq)} + 3\ H_2O \qquad (3)$$

$$8\ H^+_{(aq)} + \ Al^0 + CrO^{2-}_{4\,(aq)} \rightarrow Al^{3+}_{(aq)} + Cr^{3+}_{(aq)} + 4\ H_2O \qquad (4)$$

$$Al^{3+}_{(aq)} + \ PO^{3-}_{4\,(aq)} \leftrightharpoons \ AlPO_4 \downarrow \qquad K_s = 6{,}3 \cdot \ 10^{-19} \qquad (5)$$

$$Cr^{3+}_{(aq)} + \ PO^{3-}_{4\,(aq)} \leftrightharpoons \ CrPO_4 \downarrow \qquad K_s = 2{,}4 \cdot \ 10^{-23} \qquad (6)$$

As it can be observed, aluminium oxide is dissolved in an acid medium allowing the bath solution to reach the aluminium substrate. When this happen, a reduction-oxidation reaction, between this one and the chromic acid present in the medium, takes place. Aluminium is oxidized to aluminium (III) meanwhile chromium (VI) is reduced to Chromium (III).

Interaction between those metals in solution and the phosphate anions coming from the phosphoric acid, favours the precipitation of chromium phosphate (solubility constants) above

the piece's surface, stopping the reaction between the metal and the chromic acid. Actually, chromium phosphate is known as a good corrosion inhibitor [11].

1.5.2. Alternative method.

As it has been previously mentioned, chromium (VI) compounds are being restricted by legislation. Thus, new alternatives with new compounds have to be developed to reach the same the properties than using chromium (VI) compounds.

Several researches have shown the great properties of potassium permanganate as a good corrosion inhibitor and its chemical similarities to chromium (structural and electronic) [12, 13]. Besides, the use of fluorhydric acid as a good solvent of aluminium oxide has also been studied [14].

With all this, different bath compositions will be studied in this research project in order to obtain the most similar results than the ones with the phosphoric-chromic solution used in the industrial field as a deanodizing bath.

With those compounds in solution, reactions which could take place are the next ones:

$$Al_2O_3 + 6\,H^+_{(aq)} \rightarrow 2\,Al^{3+}_{(aq)} + 3\,H_2O \qquad (7)$$

$$4\,H^+_{(aq)} + Al^0 + MnO^-_{4\,(aq)} \rightarrow Al^{3+}_{(aq)} + MnO_2 \downarrow + 2\,H_2O \qquad (8)$$

$$Al^{3+}_{(aq)} + PO^{3-}_{4\,(aq)} \leftrightharpoons AlPO_4 \downarrow \qquad K_s = 6{,}3 \cdot 10^{-19} \qquad (9)$$

$$Al^{3+}_{(aq)} + 4\,F^-_{(aq)} \leftrightharpoons [AlF_4]^-_{(aq)} \qquad K_d = 10^{-19{,}8} \qquad (10)$$

As it has been previously shown, aluminium oxide is dissolved in an acid medium allowing the bath solution to reach the aluminium substrate. When this happens, a reduction-oxidation reaction, between this one and the manganese permanganate present in the medium, takes place. Aluminium is oxidized to aluminium (III) meanwhile manganese (VI) is reduced to manganese (II) which is insoluble, so it will be precipitate as manganese dioxide. This precipitate

will cover lightly the alloy surface stopping the reaction between the metal and the compounds in solution [13].

Fluoride anions complex the aluminium (III) coming from the oxide layer dissolution. This coordination impedes the precipitation of aluminium phosphate over the alloy's surface, due to their lower dissociation constant.

Although the influence of pH in experiments has not shown significant corrosion influence by itself in short-term exposures of alloys [15], is important to take into account the effect of the deanodizing medium pH value. It is known that potassium permanganate is a very strong oxidant when it is under a low pH medium, being able to reduce itself into Mn^{2+}. In the opposite sense, when it is under a basic medium it is not as strong oxidant, but it is still a great oxidant compound, being able to reduce itself into MnO_2 [1]. These properties of potassium permanganate could also be studied and applied during the realization of this work. The pH value could be able to control the velocity of the deanodizing process, due to the behaviour of the acids and the potassium permanganate that are being used.

1.6. Techniques used to perform analysis.

1.6.1. Inductively Coupled Plasma Atomic Emission Spectroscopy (ICP-AES).

Plasma is one of the four fundamental states of matter. It consists in a "partially ionized gas with a high temperature able to atomize, ionize and excite the majority of the elements of the periodic table" [16]. There are several atomic emission spectroscopy techniques using plasma to produce excited atoms and ions, such as Direct Current Plasma (DCP), Microwave Induced Plasma (MIP) or Inductively Coupled Plasma (ICP) among others. In the case of this work, ICP, which is a type of emission spectroscopy which uses a plasma, generated by electromagnetic induction, to excite atoms and ions in order to generate an electromagnetic radiation at the characteristic wavelengths of a particular element. This technique will be employed to perform the analysis of industrial deanodizing baths.

Inductively coupled plasma atomic emission spectroscopy (ICP-AES), also known as inductively coupled plasma optical emission spectrometry (ICP-OES), is one of the most widely used analytical techniques to perform elemental analysis and for the detection of trace metals, with great advantages such as low susceptibility to chemical interferences due to its high temperature ranges (it can reach 10000 K) and the very high quality of the spectra obtained, being possible the recording of multiple spectrum from dozens of elements present in very small samples. It also presents a high analytical sensitivity, a wide linear dynamic range and a high sample throughput [16].

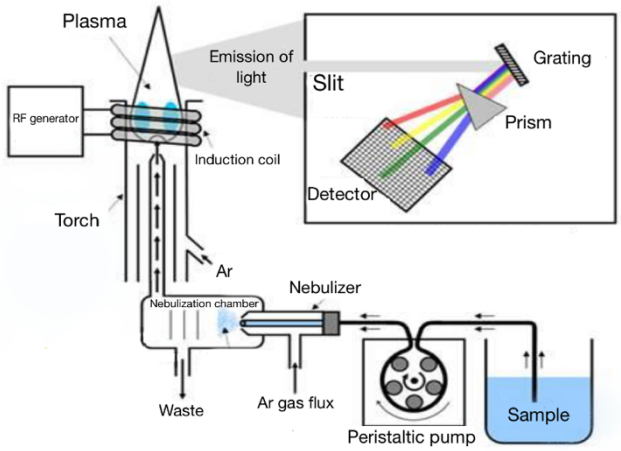

Figure 4. ICP-AES instrumentation.

As it is showed in the figure, instrumentation of an ICP-AES equipment is quite simple. The sample is introduced in an aqueous solution through a venturi effect based nebulizer with the help of a peristaltic pump. The smallest particles present in the nebulization chamber go through the torch in which they are excited emitting light. This emission will be reach the detector and transformed in an electric signal.

Selecting the correct wavelength and the optimum parameters, it is possible to quantify the elements present in the industrial baths used in this research project.

1.6.2. X-Ray Photoelectron Spectroscopy (XPS).

Electron Spectroscopy Techniques are based on the measurement of the kinetic energy of the electrons ejected from the atoms of the sample surface after their interaction with an incident beam of photons or with electrons. The most important ones are shown in the *figure 5*.

The first one, X-ray Fluorescence (XRF) consists in the emission of characteristic fluorescent X-rays from a material previously excited by bombarding it with high-energy X-rays. This phenomenon is widely used for both elemental and chemical analysis.

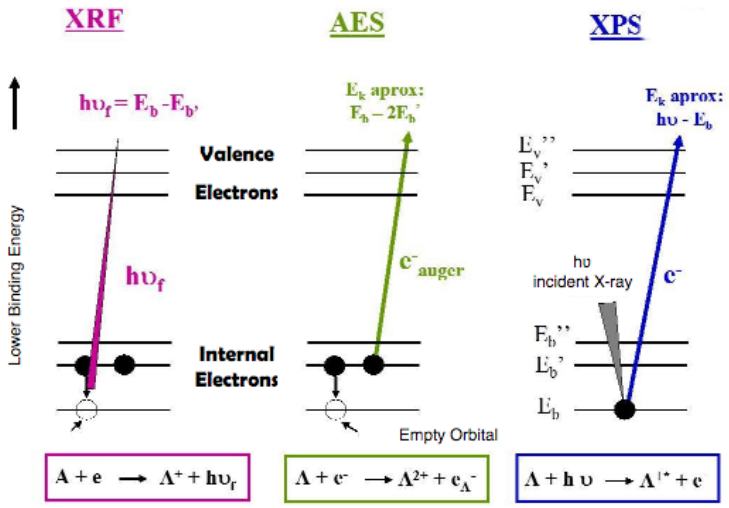

Figure 5. Different electronic phenomena in electron spectroscopy techniques.

The second one is Auger Electron Spectroscopy (AES). In this technique the surface to be analysed is irradiated with a beam of electrons with a quantity of energy enough to be able to ionize one or more core levels in the atoms of the sample surface. This process involves the participation of three electrons:

1. Initially, an electronically excited ion is form after the emission of an electron.
2. Then, the relaxation of the excited ion occurs through the fall of an outer electron to fill the gap created.
3. Finally, a third electron takes the difference of energy to scape from the atom. This electron, (Auger electron) will reach the detector.

This process has a great importance. The Auger energy only depends on the atomic energy levels. Since is not possible to find two elements with the same set of atomic energies, the analysis of Auger energies leads to the identification of the corresponding element. Because of this, it is a widely used analytical technique in the study of surfaces and, generally, in the area of materials science.

The third one, X-ray photoelectron spectroscopy (XPS), is an analytical technique based on the analysis of the electrons emitted from a solid surface after its interaction with an incident beam of X-ray photons. From XPS analysis, spectra are obtained. One XPS spectrum shows the

distribution of ejected electrons from certain atomic levels of the sample as a function of their kinetic energy or their binding energy to the atom. Some of these electrons, usually, are Auger electrons due to the process explained before.

Kinetic energy (E_c) of the emitted electrons varies by modifying the energy of the incident X-ray beam ($h\upsilon$). This energy must be greater than the electron binding energy (E_b). Its value depends on the material to be analysed itself and on the instrument (ϕ).

$$E_c = h\upsilon - E_b - \phi \qquad (11)$$

Two electrons never share the same set of binding energies. Thus, the measurement of the photoelectron E_c allows the directly and unequivocally identification of the energy of the atomic orbitals and, consequently, the corresponding element.

XPS spectra provide valuable chemical information. Changes occurring in E_b will be reflected in E_c, so it is possible to follow changes in the chemical environment of an atom through the changes observed in the photoelectron energy. Thus, this is a great analytical technique to perform Qualitative Analysis in solid samples.

1.6.3. Chromatic Confocal Microscopy (CCM).

Chromatic Confocal Microscopy (CCM) is a type of fast three-dimensional microscopy that enables high-speed three-dimensional surface profiling without mechanical depth scanning based on an optical triangulation method [17].

With this technique it is possible to carry out measurements of loss of height in solid samples such as the ones which are going to be studied during the realization of this research. Measuring this loss of height, it is possible to determine the grade of stripping of the target alloy, and, consequently, the efficacy of the treatment performed.

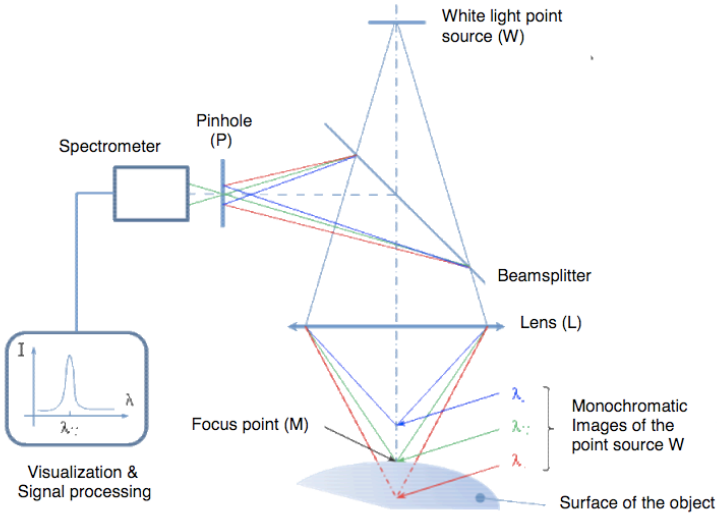

Figure 6. Instrumentation of a CCM [Stil S.A.].

As it is showed in the figure, the principle of the CCM technique consists in a polychromatic light coming from a white light point source which is focused by the objective lens towards a solid sample. Due to the various focal lengths displayed in the instrument, a vertical line with a rainbow-colour is formed at the object space. Reflected light from the sample is then directed to the pinhole after being reflected by the beam splitter. Light with a specific wavelength, which forms a focal point on the sample surface, passes through the confocal pinhole. The remaining light with other wavelengths that form focal points off from the sample surface is blocked by the pinhole. Thus, it is possible to perform the measurement of the height of a solid sample by analysing the colour of the returning light. The peak wavelength that corresponds to the height of the sample needs to be identified. To perform this identification, it is employed a spectrometer [17, 18].

1.6.4. Linear sweep voltammetry (LSV).

The corrosion resistance, or in other words, the resistance against electrochemical oxidation of alloys studied in this work is one of the most important characteristics of them. The goal of anodizing is giving to the alloy the best protection against corrosion with the purpose of keeping the aluminium substrate intact.

The most fundamental measurement of the corrosion rate is the metal weight loss rate, ΔW ($mg/cm^2/d$). This can be converted to an average corrosion rate (mm/y) using

$$P_W = 3.65\ \Delta W/\rho \qquad (12)$$

were ρ is the metal density (g/cm^3) [19].

For aluminium alloys, corrosion rates can be evaluated by Tafel extrapolation from intensity current – potential (i-E) curves. In this work, the corrosion potential of the alloys studied will be measured with the carrying out of a lineal voltammetry in an electrochemical cell which contains a working electrode which will be the alloy under study.

Linear sweep voltammetry is a voltammetric method where the applied potential between the working electrode and a reference electrode sweeps linearly under constant velocity. [20] In the case of this work, a rotating ring-disk electrode will be used, being the alloy the electrode itself. With this technique, a i-E curve will be obtained and the potential when the current intensity value is zero will be registered through the Tafel extrapolation.

When an alloy has a protective layer, the corrosion resistance is higher than in other alloy with the metallic substrate in contact with the air. Thus, the potential rate when the current intensity value is zero, E(i=0), is higher in the first case due to the requirement of more energy to be oxidized than in the second case. So, making a comparison between different treated alloys, it is possible to know how much protected is one piece and to conclude if it has been stripped from its protective layer or not.

Tafel method has a big importance in the corrosion of materials study. From a i-E curve, representing the logarithm of the intensity current versus the potential applied a different curve is obtained. From this curve it is possible to know the corrosion intensity current (i_{corr}), the transfer charge resistance (R_{TC}) and, applying the Faraday laws, it is possible to estimate the average corrosion rate, P_W [20].

2. Objectives.

Nowadays, when the industrial deanodizing process is carried out, a bath which contains Chromium (VI) species is being used. It is known that these Cr (VI) compounds are carcinogenic and have a great importance in the environment. Legislation is forbidding the employment of this compounds in the industrial field. Thus, is necessary to develop a new deanodizing process without the employment of Cr (VI) species in it.

The main objective of this work is the development and the optimization of a new and alternative deanodizing method which does not contain any Cr (VI) compound. This main objective is approached through the following partial objectives:

- Determination of the species present in the alloy after the deanodizing process.

- Carrying out tests of dissolution in an acid medium such as H_2SO_4, HF and H_3PO_4 in order to determine which one, or which combination of them has a better role.

- Develop and carry out different experimental designs (with different parameters such as time, concentration of the acids, use of corrosion inhibitors, complexants, etc.) in order to determine the ideal composition of the deanodizing bath with the use of different analytical techniques such as XPS, electrochemistry or physical measurements such as loss of weight or roughness.

3. Experimental.

3.1. Reagents and materials.

Aluminium 2024-T3 alloys after OAC and OAS process were sourced from IRT M2P (Metz, France) and used throughout all the experiments.

Reagents employed in the course of this work are the following:

- Phosphoric acid, 85%, from J.T. Baker.
- Hydrofluoric acid, 48%, reagent grade from Scharlau (Barcelona, Spain).
- Potassium permanganate, 99%, GPR Rectapur from Prolabo, VWR (Pennsylvania, USA).
- Sulfuric acid, 98%, reagent grade from J.T. Baker.
- Ultra-pure water (18 MΩ cm) obtained with a Milli-Q system (Millipore, Bedford, MA, USA).
- Phosphorus and Chromium standards for ICP-AES and ICP-MS from SCP Science (Quebec, Canada).

Material used throughout all the experiments is the general material used in a standard research laboratory.

3.2. Instrumentation.

- Activa M simultaneous CCD-based ICP-AES instrument from Horiba Scientific (Kyoto, Japan).
- Thermo Scientific K-alpha X-ray photoelectron spectrometer (XPS) from Thermo Fisher Scientific (Massachusetts, USA).
- Non-contact point CCM sensor model CHR 150-L from Stil S.A. (France).
- Transsonic Digital S ultrasonic cleaning bath from Techspan Group (Auckland, New Zeland).
- Origastat – OGS 200 potenciostat from Origalys Electrochem SAS (France).

3.3. Procedure.

Both OAS and OAC anodized aluminium alloys 2024-T3 are sourced in pieces with 95 x 120 cm dimensions. Thus, they are both reduced in the workshop until have 1.5 cm x 1.5 cm dimension pieces approximately.

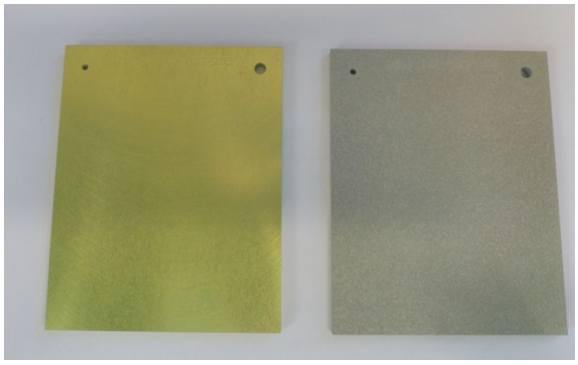

Image 1. OAS and OAC alloys studied in this work.

3.3.1. Industrial bath composition analysis.

Before beginning with the deanodizing treatment, it is necessary to know in detail the industrial bath conditions and also its composition. Thus, a calibration curve will be designed with the purpose of being analysed with the ICP-AES technique in order to know the exact concentration of the components in the industrial bath.

Solutions with 2% of acidity (instrumental conditions) of 0, 0.1, 1, 5, 10 and 20 ppm are prepared from Phosphorus and Chromium standards, in order to obtain the different points of calibration curve. Each measurement is performed in triplicate.

3.3.2. Deanodizing bath process.

Deanodizing baths are prepared in 100 mL standard volumetric flasks with the exception of solutions which contain HF. In this case, a plastic 100 mL standard volumetric flask is used due to the acid attack over the glass.

Once prepared, the solution is transferred to a 180 mL plastic container. This container is placed inside a beaker with water in order to be bain-marie-heated until reach temperatures of

approximately 90 °C under stirring conditions. When the bath temperature reaches 85 – 90 °C, the piece which is going to be deanodized is placed inside it with the help of a plastic clamp.

When a roughness measurement is going to be carried out, one half of the piece will be covered up with adhesive tape with the purpose of avoid the deanodizing in this half of the piece. With this aim, is going to be possible make a comparison between both sides and measure the difference of height between them are going to be possible, which means the loss of thickness.

When a measurement of the lost of thickness is going to be calculated by difference of weight, the piece's edges will be covered up with adhesive tape with the purpose of avoid the attack of the acids presents in the deanodizing bath over the aluminium substrate which is exposed in those edges. With the density of the alloy (d), its dimensions (b and h), the difference of weight (Δm) it is going to be possible to calculate the lost of thickness (Δw), as it is showed in the following equation:

$$d = \frac{m}{V} = \frac{m}{b \cdot h \cdot w} \Leftrightarrow w = \frac{m}{b \cdot h \cdot d} \Leftrightarrow \Delta w = \frac{\Delta m}{b \cdot h \cdot d} \qquad (13)$$

After taking control of the time that the piece has been inside the bath, it is removed from the plastic container and transferred to another one which contains distilled water with the purpose of clean it and remove the remainder acids or deanodizing bath compounds. This step is repeated in order to get a better cleaning up.

Sometimes the employment of an ultrasounds bath is necessary in order to remove the oxide layer which covers the alloys after being deanodized. Thus, the piece is immerged in a 60 mL plastic container filled up with distilled water and placed inside the ultrasonic cleaning bath during one minute.

3.3.3. XPS analysis.

Pieces which are going to be analysed with the X-ray photoelectron spectroscopy (XPS) need to have a great cleaned up before being brought in the instrument. To do that, pieces have to be placed in the instrument's sample holder being necessary the establishment of an electrical connexion between it and the samples with the purpose of avoid interferences.

Once the pieces are placed in the sample holder, it is introduced in the low vacuum chamber passing through an inert atmosphere pre-chamber. When the low vacuum values are achieved, the sample holder is introduced into the high vacuum chamber and when the pressure reaches lower values than 10^{-9} bar and they are stable, the XPS analysis begins.

Before starting, a general sweep from the lowest until the highest binding energies has to be performed. With this aim, a general view of the components will be given and it will be possible to select those peaks under interest in order to elucidate the exact composition and its abundance in the sample it is being analysed. This composition has an uncertainty of 0.01 %.

3.3.4. Roughness measurements (CCM).

Evolution of thickness and roughness of half deanodized pieces are studied with this technique. Pieces with two sides, one after deanodizing and the other one without any treatment after the industrial anodizing process are employed in order to compare both sides between them. In addition, evolution of thickness during deanodizing and the roughness of the deanodized part of the piece are quantified with this technique.

To do that, the sensor is placed in the border between the two sides and 1.5 mm of each one is measured, beginning from the anodized side until reach the deanodized one. With this, a curve with the height difference between both sides and the roughness values are obtained.

3.3.5. Electrochemical corrosion measurements.

In order to carry out the electrochemical measurement of corrosion, the following instrumentation is used.

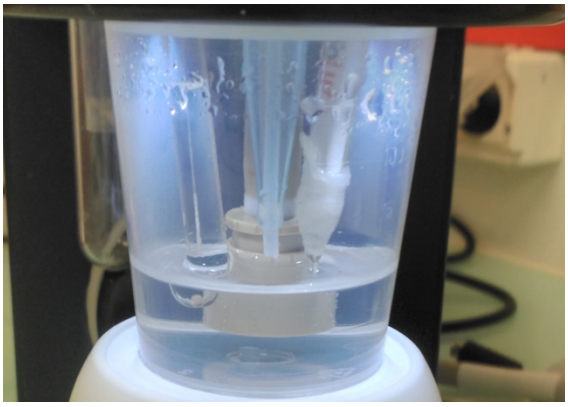

Image 2. Set up of the electrochemical cell.

In the *image 2*, it is possible to see a typical electrochemical set up instrumentation. Beginning from the left side, there is placed the reference electrode (Ag/AgCl electrode with an internal solution of KCl 1M). In the middle of the set up, it is possible to see the working electrode inside the plastic structure. In front of the working electrode, a capillary is placed with the aim of introduce nitrogen and avoid the presence of oxygen in the solution. Finally, on the right side, it is possible to see the auxiliary electrode (Pt). The intensity current is measured between the working electrode and the auxiliary one, meanwhile the potential is measured between the reference electrode and the working one. A solution of NaCl 1% (w/w) is used to carry out the measurements and a potential sweep is made from -1.6 V up to +1.6 V with a speed of 10.021 mV/s.

4. Results and discussion.

4.1. Industrial bath composition analysis.

4.1.1. Phosphoric acid concentration.

The following calibration curve is obtained measuring at the maximum intensity of emission of Phosphorus (λ_p = 177.433nm).

Table 4. Calibration.

Conc.	I(177.433nm)
0	0
0.1	21.473
1	229847
5	1183.302
10	2400060
20	4701.430

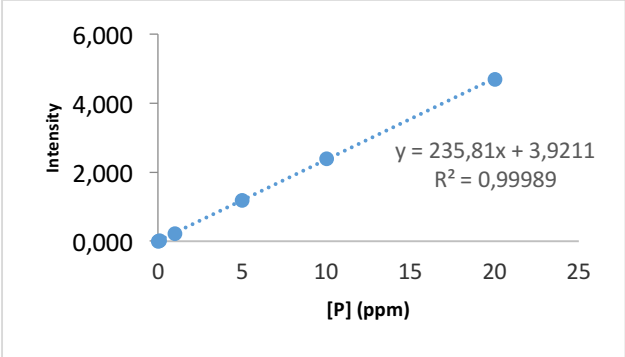

Graphic 1. Calibration curve of Phosphorus at 177,433 nm.

Three different diluted aliquots (1:100, 1:1000, 1:1000) have been analysed since it is not known its real concentration. The one or ones which fit in the calibration curve will be used to quantify the composition of phosphorus in the sample.

Table 4. Results from the calibration curve.

	1:100	1:1000	1:10000
Intensity	35187.984	3597.809	356.265
RSD(%)	0.87	0.49	0,75
Diluted concentration	149.2079	15.24097	1.49421
Concentration (ppm)	-	15240.9711	14942.1346

➔ Taking both dilutions into consideration, concentration of phosphorus and therefore, concentration of phosphoric acid in the sample is 0.487 ± 0.007 M.

4.1.2. Chromic acid concentration.

The following calibration curves are obtained by measuring at the two maximum intensity of Chromium.

For the measurements at λ_{Cr}= 205.571 nm:

Table 5. Calibration curve data.

Conc.	I(205.571nm)
0	0
0.1	233.276
1	2450.042
5	12466.594
10	24705.000
20	49177.949

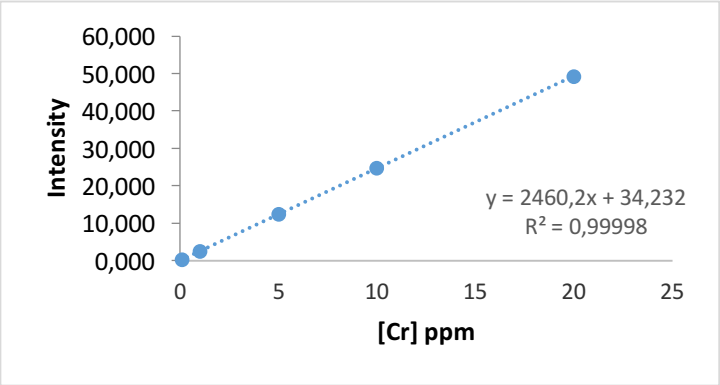

Graphic 2. Calibration curve of Chromium at 205,571 nm.

Table 6. Results from the calibration curve.

	1:100	1:1000	1:10000
Intensity	287333.508	30794.185	3020.104
RSD(%)	0.16	1.27	0.79
Diluted concentration	116.7773	12.5020	1.1213
Concentration (ppm)	-	12502.03	1.2127

For the measurements at λ_{Cr}= 267.719 nm:

Table 7. Calibration data.

Conc.	I(267.719nm)
0	0
0.1	16911.721
1	166954.307
5	897333.970
10	1788814.133
20	3500115.415

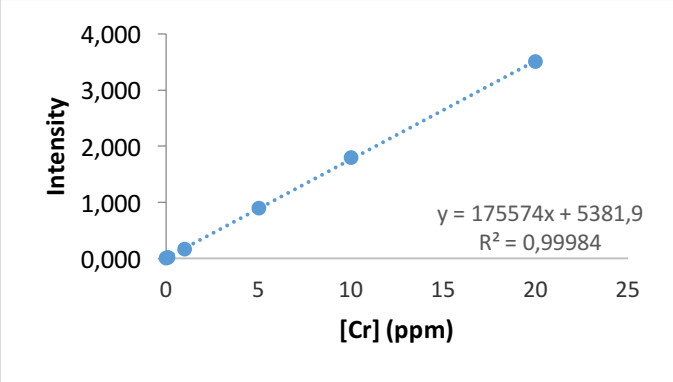

Graphic 3. Calibration curve of Chromium at 267,719 nm.

Table 8. Results from the calibration curve.

	1:100	1:1000	1:10000
Intensity	20295675.336	2124982.158	207982.532
RSD(%)	0.20	0.73	1.98
Diluted concentration	115.5656	12,0728	1,1543
Concentration (ppm)	-	12072.7561	11543.068

➔ Taking all the four dilutions into consideration in the two wavelengths, concentration of chromium and therefore, concentration of chromic acid in the sample is 0.232 ± 0.008 M.

4.2. XPS analysis of the alloys under study.

The composition of the two type of pieces which are used during all this work through the different deanodizing bath compositions (OAC and OAS ones) has been determined with the X-ray photoelectron spectroscopy (XPS) technique, with the purpose of having a reference from where make a comparison between the pieces after the different deanodizing baths with the aim of knowing if the deanodizing process has been achieved.

For the analysis of one chromic acid anodized piece, the spectrum obtained, and from it, the chemical composition results are the next ones.

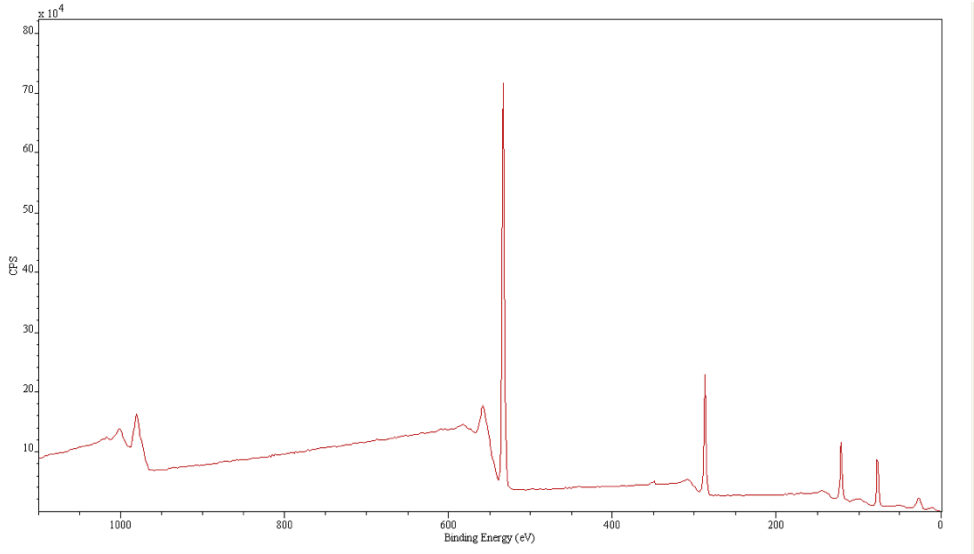

Graphic 4. XPS spectrum of a OAC piece.

From this spectrum the most important peaks were analysed and both, them and their respective concentration, are detailed in the following table.

Table 9. Composition in % of a chromic anodized piece analysed with XPS (% ± 0.01 %).

Name	*Al 2p*	*Cu 3p*	*C 1s*	*C 1s*	*C 1s*	*Ca 2p*	*Ca 2p*	*O 1s*	*O 1s*
B.E. (eV)	75.160	77.223	285.00	286.03	289.04	347.60	351.16	532.33	530.96
% Conc.	14.84	2.27	23.73	4.49	1.85	0.26	0.14	36.20	16.22

In the Handbook of the Elements and Native Oxides, it is possible to find a relationship between the binding energy of the peaks and its composition. In all the XPS spectrum they are always found a very tall peak corresponding to Oxygen, and another one corresponding to Carbon. Theses big amounts of C and O correspond to different esters, ketones and other compounds which are present in the surface of the sample as organic contaminants. From peaks corresponding to the aluminium 2p and the oxygen 1s (523.33 eV) it is possible to check that both species could correspond to the Al_2O_3 compound, which has a logical meaning, and if their compositions are added, it results a 51.04 % of Al_2O_3 over the sample's surface. Different forms of Ca (some residues over the piece's surface) and Cu (typical element present in 2024-T3 alloys) are also found.

With the analysis of the sulfuric acid anodized piece, the spectrum obtained and the results from it are quite different than in the previous sample.

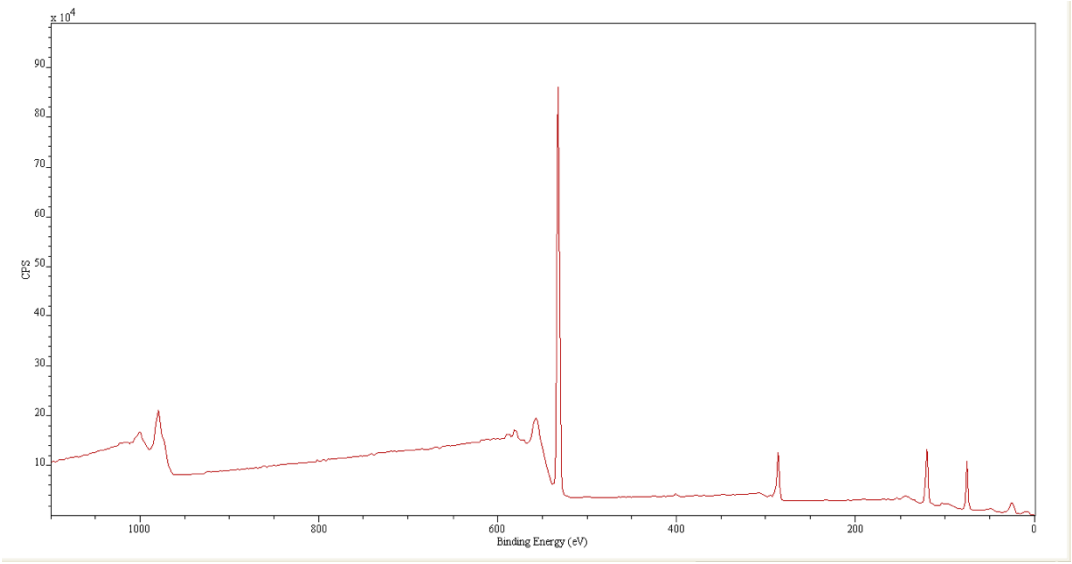

Graphic 5. XPS spectrum of a OAS piece.

Table 10. Composition in % of a sulfuric anodized piece analysed with XPS (% ± 0.01 %).

Name	*Al 2p*	*C 1s*	*C 1s*	*C 1s*	*Cr 2p*	*N 1s*	*O 1s*	*O 1s*	*S 2p*
B.E. (eV)	74.32	285.00	286.25	289.32	577.62	399.99	532.20	530.76	168.78
% Conc.	27.66	10.16	4.36	1.56	0.47	0.56	38.98	15.02	0.20

Although in this case most of the compounds are the same ones than in the previous analysis, such as the presence of Al_2O_3 that in this case has a value of 66.64 (this difference of composition between the previous analysis could be due to the lower contamination from carbonated compounds, as it can be observed in the spectrum, that the peak corresponding to C has a lower intensity). It could be found the presence of Chromium. If the Handbook of the Elements and Native Oxides is checked, it can be concluded that this Cr present in the sample corresponds to the Cr (III) which is used in the sealing process of anodized pieces and it does not correspond with Cr (VI) (it appears at 579.5 eV). Other elements such as sulfur (coming from the bath composition), and nitrogen (contamination) are found in the sample.

With all this data, making a comparison with the deanodized pieces, it is possible to see the presence of different compounds after deanodizing and determine if the process has been successfully achieved or not.

4.3. Optimization of temperature.

In order to know and achieve the best temperature conditions, different deanodizing baths are prepared. To do that, different temperatures and different compositions are employed. All the bath compositions and their results are detailed in the *Annex 1* due to the big amount of them.

Considering the industrial deanodizing bath conditions, the first experiments are carried out by using phosphoric acid as principal compound in the bath due to its strong corrosiveness on aluminium and its alloys [21], potassium permanganate to avoid the attack of the acid over the aluminium substrate and under room temperature conditions [22]. The concentration of phosphoric acid has been chosen keeping in mind the industrial bath concentration of this acid. A lower concentration was chosen in order to evaluate the influence of this acid during the deanodizing and his effects. Concentration of potassium permanganate is quite lower than the chromic acid due to its tendency to form quickly a MnO_2 layer over the piece. Thus, the concentration of $KMnO_4$ has been chosen over 0.01M approximately with small variations depending on the experimental design.

Nevertheless, nothing happens under these conditions. Thus, new bath compositions and new temperatures are employed to evaluate and optimize this last parameter.

As it can be observed in *Annex 1*, phosphoric acid is not effective at those temperatures. Therefore, sulfuric acid and the industrial bath which contains chromium (VI) compounds are also employed in order to see if deanodizing is achieved with another bath composition. Seeing than nothing happens, the temperature is increased until reach the 80 – 85 °C when deanodizing is achieved. Temperatures over 80 – 90 °C can not be reached due to instrumental limitations.

At this temperature, with H_3PO_4, the deanodizing process takes place in most of the pieces, both OAC and OAS. It should be pointed out that the anodic layer from pieces treated under sulfuric acid anodizing process are removed faster than the ones treated under chromic oxide anodizing process. In addition, by using H_2SO_4 instead of H_3PO_4, anodic layers from OAS pieces are still being removed, meanwhile, apparently, anodic layers in OAC pieces are not removed. The reactions which take place during this process have been explained in section 1.5.2. from equation 7 to equation 10.

It can be seen that brown or black layers appear over the pieces after deanodizing in some cases. Its composition will be studied with XPS.

4.4. Industrial deanodizing process references.

In order to have a starting point and a reference of deanodized piece, different experiment with industrial deanodizing baths are going to be performed at different times of immersion of each piece. Two baths with only phosphoric acid will be prepared and one bath with the industrial deanodizing composition in order to compare with the other results and to have a reference of an anodized piece. Reactions which take place in this process are explained in section 1.5.1.

Once the pieces have passed through each bath, the corrosion potentials of each one, a study of the roughness and loss of weight is performed with the CCM, and also a study of the composition of each one with the XPS technique.

A measurement of the evolution of thickness and the roughness was done to pieces whose deanodizing conditions detailed in the following tables.

Table 11. Different conditions of deanodizing OAC pieces and their respective loss of thickness and roughness results.

	10 min		20 min		30 min	
OAC	**Evolution of thickness (µm)**	**Roughness (µm)**	**Evolution of thickness (µm)**	**Roughness (µm)**	**Evolution of thickness (µm)**	**Roughness (µm)**
H_3PO_4 0.2M	-3.74	0.606	-7.45	6.25	-12.4	14.1
H_3PO_4 0.5M	-4.71	0.888	-13.5	1.13	-16.4	6.34
H_3PO_4/H_2CrO_4	-1.38	0.394	-2.15	0.351	-5.25	0.47

Table 12. Different conditions of deanodizing OAS pieces and their respective loss of thickness and roughness results.

	10 min		20 min		30 min	
OAS	**Evolution of thickness (µm)**	**Roughness (µm)**	**Evolution of thickness (µm)**	**Roughness (µm)**	**Evolution of thickness (µm)**	**Roughness (µm)**
H_3PO_4 0.2M	-0.882	1.23	-10.9	37.1	-7.2	23.0
H_3PO_4 0.5M	-5.89	0.563	-16.6	14.9	-14.2	42.8
H_3PO_4/H_2CrO_4	-1.36	0.968	-7.76	1.25	-7.83	27.7

As it can be observed, in both cases the general tendency is to decrease the thickness and increase the roughness due to the more time inside the bath under the attack of the acids present.

A measurement of the corrosion potential values was also carried out with the electrochemical techniques. They are compared between themselves the two pieces after and before deanodizing bath and between a piece of pure aluminium as well.

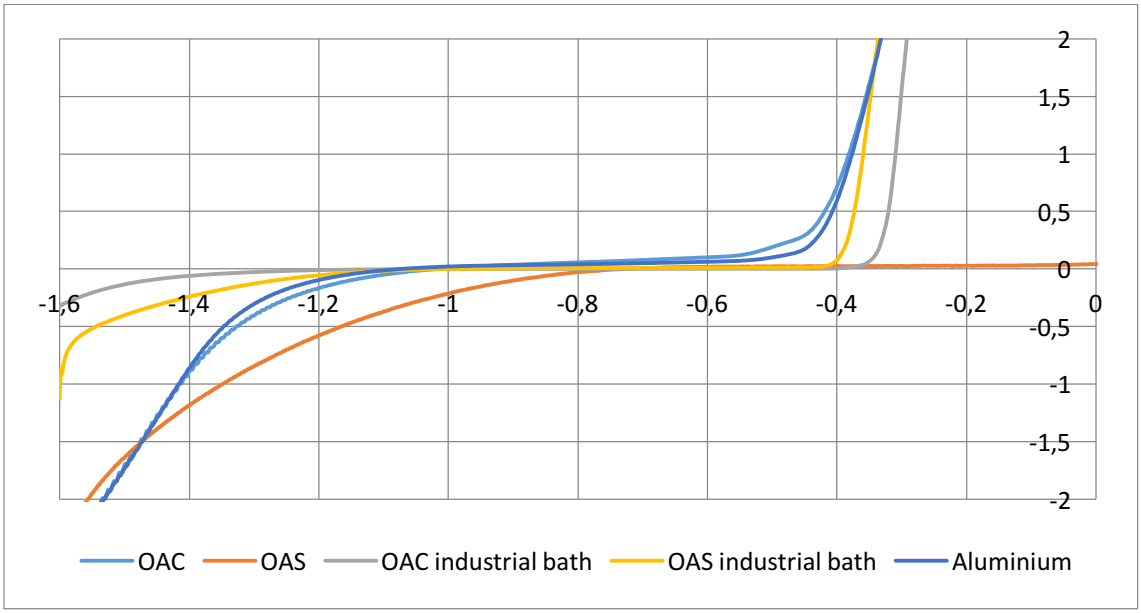

Graphic 6. i-E curves from different analysed pieces.

From curves i-E of graphic 6 it is possible, with the Tafel extrapolation, to know the corrosion potential values of each piece.

Table 13. Potential rates vs $E_{Ag/AgCl}$ when the density of current is zero.

OAC	**OAS**	**OAC industrial**	**OAS industrial**	**Aluminium**
-304.1 mV	-736.8 mV	-937.3 mV	-972.3 mV	-1077.5 mV

From this table, it is observed than, the less protection that pieces have, the lower is the potential when the current intensity is zero, even though with the industrial bath, the value from stripped aluminium is not reached.

4.5. Evolution of the parameter's influence over the deanodizing process.

Once the temperature has been optimized and fixed, the effect and the influence of other parameters such as duration of the process and different compositions of the deanodizing bath have to be studied and optimized with the development of different experimental designs.

In an experimental design, different parameters were studied. Therefore, each parameter must have two different values: one high and one low. These values are compared with the ones of other parameters. As it has been explained in section 4.3., the concentration of H_3PO_4 has been selected keeping in mind the industrial bath concentration of this acid. A lower concentration was selected in order to evaluate the influence of this acid during the deanodizing and his effects. The effect of HF as a solvent of the anodized layer and complexant has been also studied as it has been explained in section 1.5.2.

Concentration of potassium permanganate is quite lower than the chromic acid due to its tendency to form quickly a MnO_2 layer over the piece. Thus, the concentration of $KMnO_4$ has been selected over 0.01M approximately with small variations depending on the experimental design.

The pH of the medium has been also considered as an important parameter. With different pH values a different attack is obtained over the piece and a different behaviour is observed in $KMnO_4$ as it has been explained in section 1.5.2.

With all of this, it is possible to determine the influence of each parameter such as concentration of different acids, time of immersion, etc. over the alloy with the purpose of finding the best deanodizing bath composition.

4.5.1. Optimization of time.

Different experiences were carried out in order to determine the time during which pieces are immerged in the deanodizing bath. Within this experiments, behaviour of 32 pieces of both OAC and OAS alloys were studied under different conditions which are detailed in *Annexe 2.*

Sixteenth pieces of each anodizing method were under study. However, as it was found out before, time between chromic anodized and sulfuric anodized pieces is different because anodic layer from OAS pieces are removed easier and faster than the OAC ones. Thus, for chromic anodized pieces the time varies from 10 up to 20 minutes, and for sulfuric anodized pieces, from 5 up to 20 minutes.

Dimensions of each piece were measured before beginning the treatment in order to calculate its thickness with *Eq. 13*. After the deanodizing bath, pieces were measured once again with the purpose of estimate the loss of thickness of each piece during the treatment.

Graphic 7 shows the loss of thickness of each piece, corresponding the green bars to sulfuric oxide anodized pieces and the grey bars to chromic oxide anodized pieces.

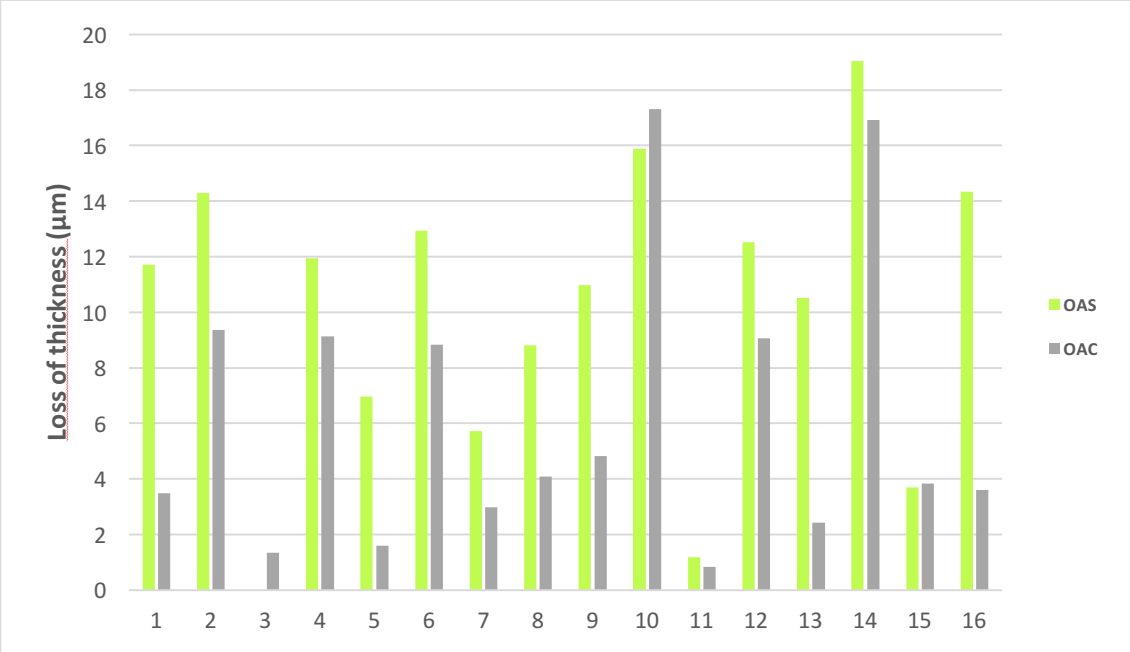

Graphic 7. Loss of thickness of pieces from the first experimental design.

The biggest evidence that can be observed is that, with the exception of a few cases (experiments 3, 11 and 11), even with a lower time immerged within the deanodizing bath, sulfuric acid anodized pieces loose a wider layer than chromic anodized ones.

It is also an evidence that the more time that pieces are under deanodizing bath conditions, the bigger loss of thickness is achieved on the pieces. It is shown between pieces from 1 and 8, and from 9 and 16.

Small differences could be found between this results and the results obtained with the chromatic confocal microscope concerning the evolution of thickness. This differences can be caused by a non perfect protection given by the adhesive used to cover the edges of the pieces. This could allow an attack from the acids to the aluminium present in those edges, giving a higher loss of weight and, consequently, a mistake in the estimation of loss of thickness.

In order to clarify and discover the influence of each parameter under deanodizing results, a studio of the influence of each parameter of the experience design was done and its results are showed in *Graphic 8*.

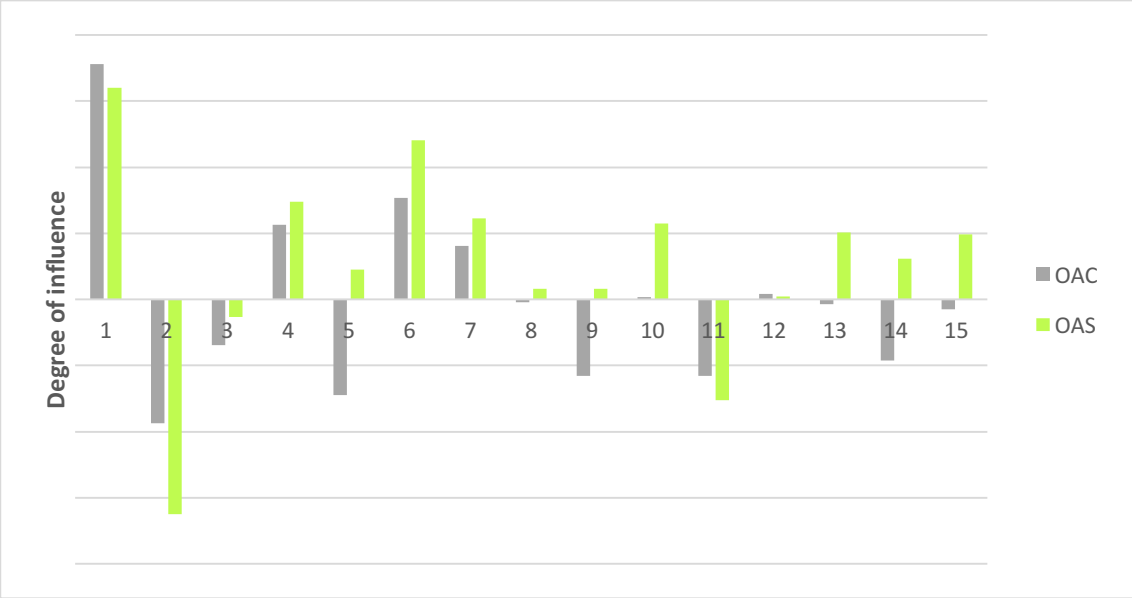

Graphic 8. Degree of influence of each parameter during the first experimental design

Parameter	1	2	3	4	5	6	7	8	9	10	11	12	13	14	15
Experience	**(1)**	**(2)**	**(3)**	**(4)**	**(12)**	**(13)**	**(14)**	**(23)**	**(24)**	**(34)**	**(123)**	**(234)**	**(134)**	**(124)**	**(1234)**

In this graphic, over the Y-axis is represented the degree of influence. The more positive the bar is, the more important influence that its parameter has with deanodizing. So, if in this case, the parameter increases its value or its concentration, deanodizing is more effective and a bigger loss of thickness is achieved. To the contrary, when some bars are negative, it means that those parameters have a negative influence with deanodizing, that is to say, anodizing is stronger avoided when the parameter increases its concentration or value. In the X-axis are shown the different parameters under study and their combination between themselves.

Number 1 corresponds to [H_3PO_4], number 2 to pH, number 3 is [$KMnO_4$] and number 4 is for the time. The next ones are the combination between them as it is explained underneath the graphic.

So, for all the above reasons, it could be come to the conclusion that, as phosphoric acid concentration and duration of the process are the most influence parameters over deanodizing, pH and permanganate concentration, this one less significant than pH, are the parameters which more slow down the deanodizing process over the pieces.

A XPS analysis were carried out with pieces 1 and 10 from this experimental design (the apparently best deanodized ones). They correspond to the bath containing H_3PO_4 0.2M and the lower time in the bath for experiment 1; and H_3PO_4 0.5M and the higher time in the bath for experiment 10.

For pieces number one (OAC and OAS), the most relevant peaks and the composition of its elements are detailed in the following tables.

Table 14. Atomic composition in % of the most relevant peaks of a OAS piece after being deanodizing during 10 min in H_3PO_4 0.2M (% ± 0.01 %).

Peak	*Al2p*	*Cu3p*	*C1s*	*Cr2p*	*Cr2p*	*Fe2p*	*Fe2p*	*N1s*	*O1s*	*P2p*	*Zn2p*
B.E. (eV)	74.67	77.39	285.0	577.3	587.0	710.6	715.0	399.8	531.7	133.8	1022.5
% Conc.	22.87	0.65	21.26	0.33	0.19	0.39	0.20	0.67	40.51	3.12	0.30

In this case, although Al and O peaks are also found in the spectrum, they could correspond to a mixture of compounds between Al_2O_3 and $Al(OH)_3$ due to the position of the peaks in the spectrum. The presence of Cr is again standing up with a quite bigger concentration than in the anodized piece (0.05 %) which could mean that deanodizing was not successfully achieved, but it does definitively not correspond to Cr (VI) due to its binding energy. It should correspond to the Cr employed during the sealing process. The presence of Fe, Cu (in higher concentration) and Zn could be a signal of reaching the metallic surface, since they are present in the alloy 2024-T3.

For the piece one OAS, with a higher concentration of phosphoric acid and more time under the deanodizing process, the found peaks and their respective data are detailed in the following table.

Table 15. Atomic composition in % of the most relevant peaks of a OAS piece after being deanodizing during 10 min in H_3PO_4 0.2M (% ± 0.01 %).

Peak	*Al2p*	*Cu3p*	*C1s*	*Cr2p*	*Cr2p*	*F1s*	*N1s*	*N1s*	*O1s*	*P2p*	*S2p*
B.E. (eV)	74.9	77.0	285.0	577.9	587.3	685.8	400.2	401.8	532.1	134.2	168.9
% Conc.	17.00	0.62	19.97	0.33	0.20	0.26	1.79	0.20	46.10	5.03	0.55

In this case, the speciation for the Al and Cr is the same than in the previous case. Although another form of Cr has been found, it is not Cr (VI). Compounds such as P and S coming from the employed acids are also found. The high presence of Cu in this case, also could be a signal that deanodizing was achieved.

For pieces corresponding to the experiment number 10, the most relevant peaks and the composition of its elements are detailed in the following tables.

Table 16. Composition in % of the most relevant peaks of a OAC piece after being deanodizing during 20 min in H_3PO_4 0.5M (% ± 0.01 %).

Peak	*Al2p*	*Al2p*	*Cu3p*	*C1s*	*Ca2p*	*N1s*	*Na1s*	*O1s*	*P2p*	*P2p*	*Zn2p*
B.E. (eV)	74.8	72.8	77.3	285.0	347.5	400.2	1072.0	531.8	133.3	134.5	1022.2
% Conc.	37.00	2.73	4.70	11.91	0.65	0.76	0.72	21.27	1.85	0.95	0.11

Table 17. Composition in % of the most relevant peaks of a OAS piece after being deanodizing during 10 min in H_3PO_4 0.5M (% ± 0.01 %).

Peak	*Al2p*	*Al2p*	*Cu3p*	*Cu3p*	*C1s*	*Ca2p*	*F1s*	*N1s*	*O1s*	*P2p*
B.E. (eV)	75.2	73.1	77.6	79.9	285.1	347.8	685.6	400.1	532.1	133.6
% Conc.	31.96	3.14	4.36	0.67	11.93	0.62	1.20	0.79	30.32	2.65

Again for the two type of pieces, the same two different species of Aluminium are found, but it is remarkable to observe how the concentration of Cu has increased. This could mean that the metallic substrate was achieved. It is also remarkable the non presence of chromium. With the deanodizing bath, it could be possible to eliminate all the chromium present due to the sealing bath, and this is also another signal that deanodizing could be done successfully.

4.5.2. Influence of different parameters.

Once a study of the influence of the time with phosphoric acid as the only one acid in the medium has been done, a new experimental design was performed now with the purpose of evaluate its influence over the deanodizing process. Time is going to disappear from the new experimental design and HF is going to appear instead. This second experimental design was carried out with different conditions detailed in *Annexe 3*.

As it can be observed, in the first 8 experiences, the conditions are the same than in the first experimental design. Thus, those experiments will be taken into account and the new ones will be performed with a time of 10 minutes maximum, measuring also the loss of thickness at 2 and 5 minutes of deanodizing.

The loss of thickness has been calculated by using the loss of weight and the *Eq. 13* explained before. The *Graphic 9* shows the comparison of the loss of thickness between the eight first pieces from the first experimental design and the pieces from the second one.

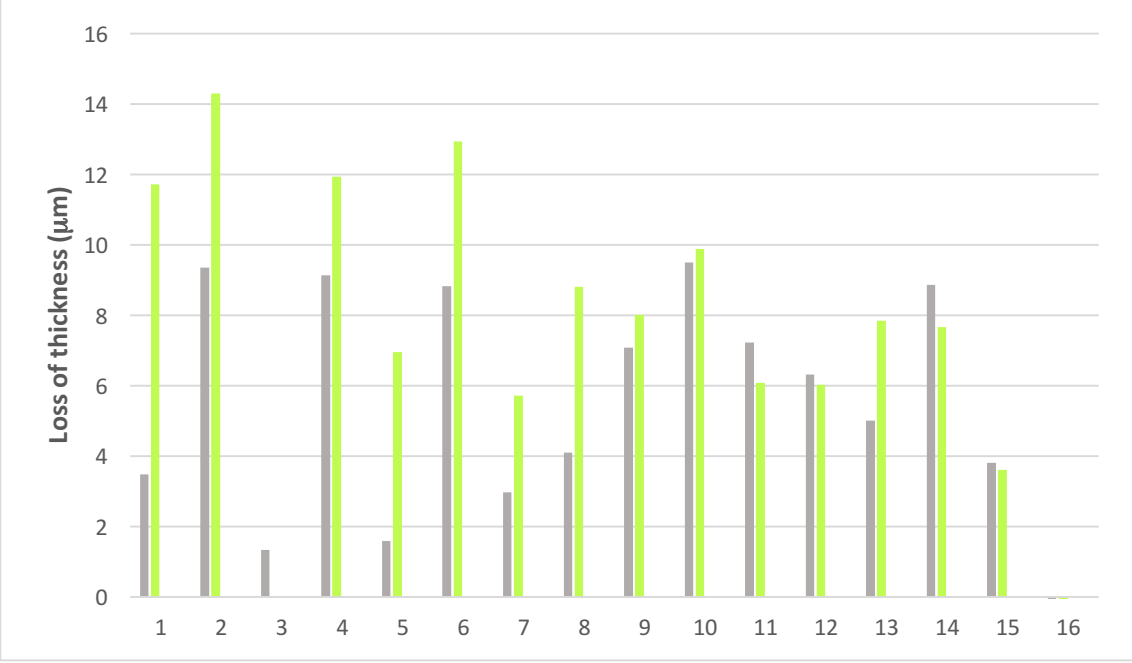

Graphic 9. Loss of thickness of pieces from the first (1 – 8) and second (9 – 16) experimental design.

When pieces are moved away from the deanodizing bath, it is possible to observe a black layer covering them. This black layer is easily removed under the effect of the ultrasonic cleaning bath in distilled water for one minute. So, as it can be observed, all the pieces under the action

of HF have been apparently deanodized, because it is possible to see the metallic substrate, apart from the last one (16), whose loss of weight has been negative.

However, data from this experimental design are not enough to evaluate the action of fluorhydric acid and which will be studied later on.

A XPS analysis of pieces 9, 11, 13, and 15 corresponding to this experimental design was carried out. In all of them, one peak corresponding with the metallic aluminium was found, and it could be a signal of the achievement of deanodizing. High concentrations of F^- were found on the surface of the piece pointing out that the HF does not only acts as a complex the aluminium but it reacts with other elements present in the alloy.

4.5.3. Influence of sulfuric acid.

After trying two different experimental designs with the use of phosphoric acid, the effect of H_2SO_4 under different conditions were evaluated in this section. The conditions and the parameters are displayed in *Annexe 4* and the time was 10 minutes per piece and bath.

In this case, the lower concentration of permanganate is not zero in order to compare different concentrations of permanganate as well as evaluate the sulfuric acid effects on the pieces during the deanodizing bath.

Dimensions of each piece were measured before beginning the treatment in order to calculate its thickness with the *Eq. 13*. After the deanodizing bath, pieces were measured again with the purpose of estimate the loss of thickness of each piece during the treatment.

Graphic 10 shows the loss of thickness of each piece, corresponding the green bars to sulfuric oxide anodized pieces and the grey bars to chromic acid anodized pieces. These values were calculated by using the *Eq. 13.*

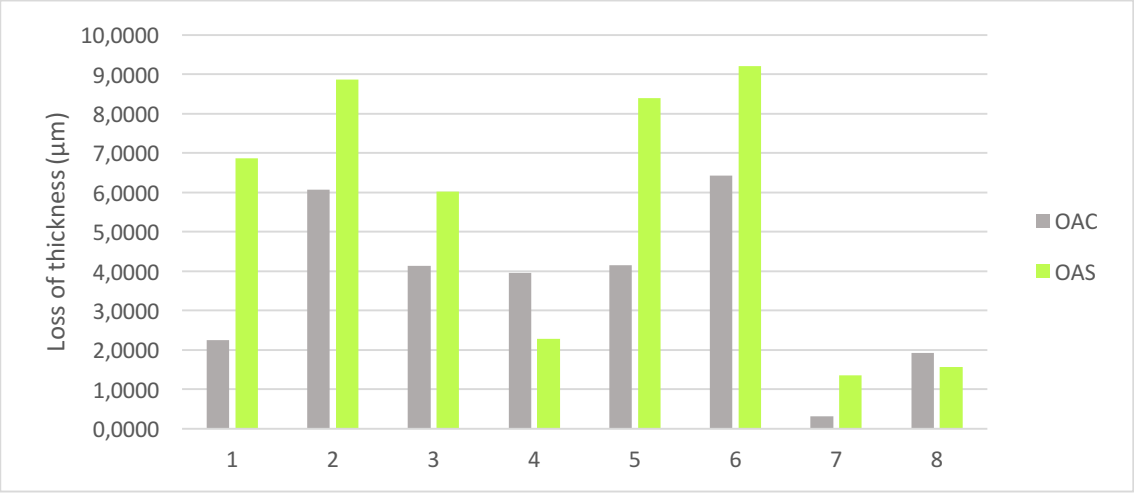

Graphic 10. Loss of thickness of pieces from the third experimental design.

Although it is possible to observe in the graphic a significant loss of thickness in most of the pieces studied, this loss is not big enough to achieve the full deanodization of the pieces. It can be seen in each piece how the anodic layer is still present.

However, a study of the influence of each parameter during this experimental design was done, being the results in the next graphic.

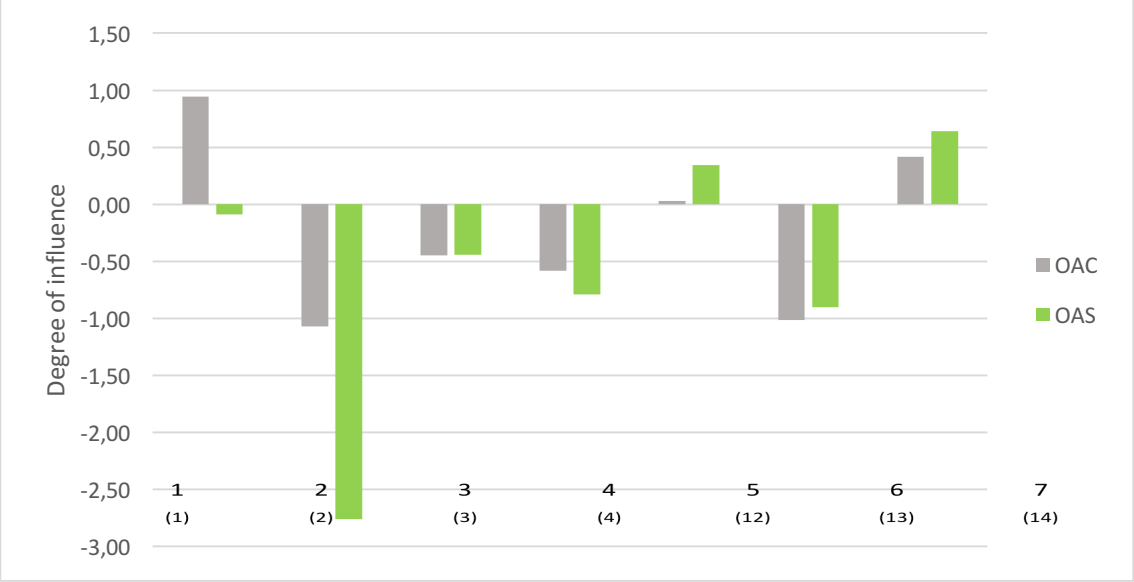

Graphic 11. Degree of influence of each parameter during the first experimental design.

In this graphic, as it was also done and explained in *Graphic 8,* over the Y-axis is also represented the degree of influence of each parameter and in the X-axis are shown the different parameters under study and their combination between themselves. Number 1 corresponds to [H_2SO_4], number 2 to pH and number 3 is [$KMnO_4$]. The following ones are the combination between them as it is explained in the graphic.

Seeing the results, it is obvious that sulfuric acid is not as effective than phosphoric acid with the same concentration levels, having the pH and the potassium permanganate the same behaviour than in the previous experiments. Thus, it is possible to conclude that the use of phosphoric acid in deanodizing baths is essential.

4.5.4. Influence of fluorhydric acid.

In order to know deeper the influence of fluorhydric acid in deanodizing baths, a new experimental design were carried out. In this design, the concentration of potassium permanganate was the same for all the different baths, and the variable parameters were the ones studied before. The difference between this experimental design and the second one is the time. Meanwhile in the second experimental design the time was not the same for all the pieces, in this one the time of immersion was over 30 minutes. The conditions of this experimental design are detailed in *Annex 5*.

From this experimental design, several analyses have been performed over different pieces. A measurement of the roughness and loss of thickness was carried out with the chromatic confocal microscope and also different electrochemical measurements were performed.

Once the pieces have been under the deanodizing bath condition during 30 minutes, they have passed through an ultrasounds bath for one minute with the purpose of remove the black layer formed over them.

For both pieces, chromic acid and sulfuric acid anodized ones, similar results were obtained after 30 minutes of treatment. A study of their evolution of thickness and roughness was carried out with the chromatic confocal microscope. The evolution of thickness results are detailed in *Graphic 12*.

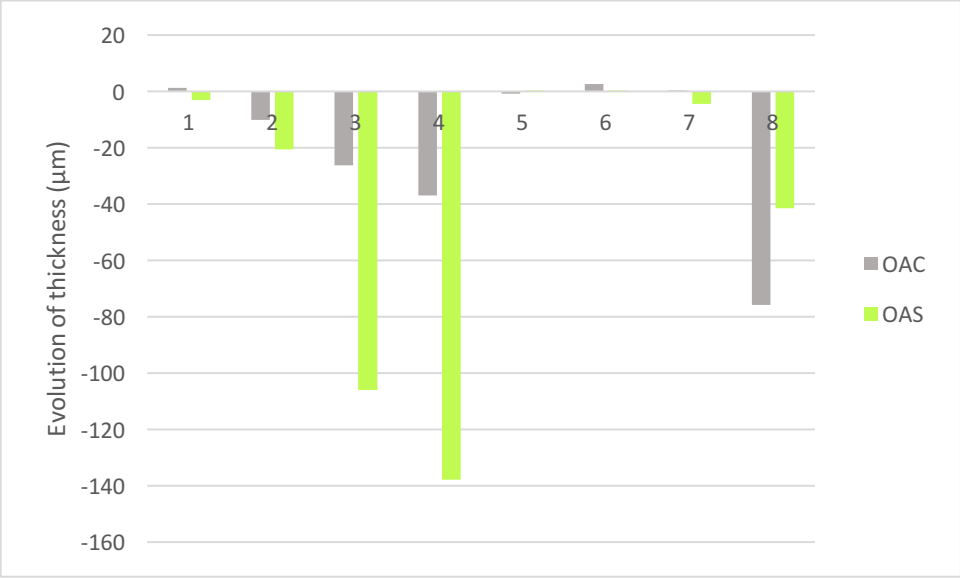

Graphic 12. Results of the measurement with the CCM of the loss of thickness of pieces from 5th experimental design.

Values from this graphic are negative. This happens because the chromatic confocal microscope gives the data in negative numbers if it has been a loss of thickness and it gives positive data if the piece has increased its thickness. The typical data obtained from CCM has the following form.

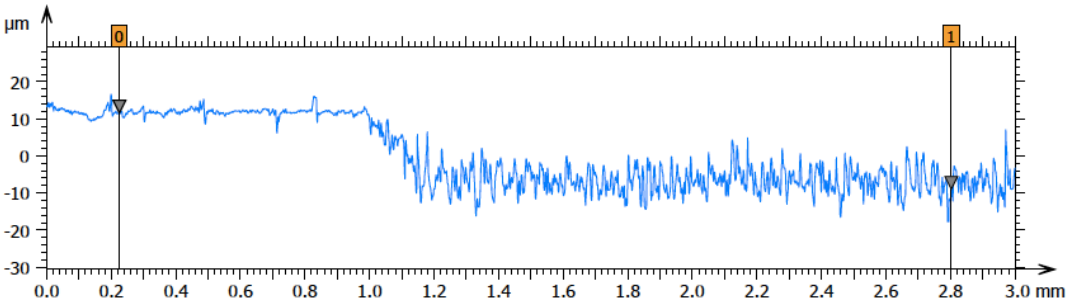

Paramètres	0-1	Unité
Distance horizontale	2.58	mm
Différence de hauteur	-20.5	µm

Graphic 13. Loss of thickness corresponding to the OAS after being treated with H_3PO_4 0.5M and $KMnO_4$ 0.01M.

For chromic acid anodized pieces, deanodizing has been achieved for the ones corresponding to the experiments 2, 3 and 4. As it can be observed, the addition of both phosphoric acid and fluorhydric acid increases the quantity of layer removed during the process. Meanwhile, for sulfuric acid anodized pieces, deanodizing has been also achieved for pieces corresponding to the experiments 2, 3 and 4. As it can be observed, although the quantity of removed layer is higher in this type of piece, the same pattern than in the previous graphic is

observed. For the pieces corresponding to the experiment 8, a permanent black layer is also covering the piece, so, as it was said before, it is supposed that deanodizing has not been achieved.

If the roughness results are also analysed, it is possible to see how it they have not the same behaviour but quite similar over pieces 2, 3 and 4 than the loss of thickness, that is to say, it increases its value with the increasing or addition of phosphoric acid or hydrofluoric acid as it can be observed in the following table.

Table 18. Roughness values from 5th experimental design obtained from the CCM.

Nº PIECE	**1**	**2**	**3**	**4**	**5**	**6**	**7**	**8**
OAC	0.431	1.76	2.27	2.08	0.358	0.27	2.09	6.55
OAS	0.466	2.66	22.9	21.4	1.09	1.8	7.57	1.5

With all these pieces, different electrochemical measurements were carried out with the purpose of determine their corrosion potential values and compare them with the metallic aluminium and the pieces after industrial deanodizing. The representation of the Tafel curves of pieces corresponding to the number 2 of this forth experimental design (H_3PO_4 0.5M and $KMnO_4$ 0.01 M), the metallic aluminium and the corresponding anodized pieces are detailed in the following graphic.

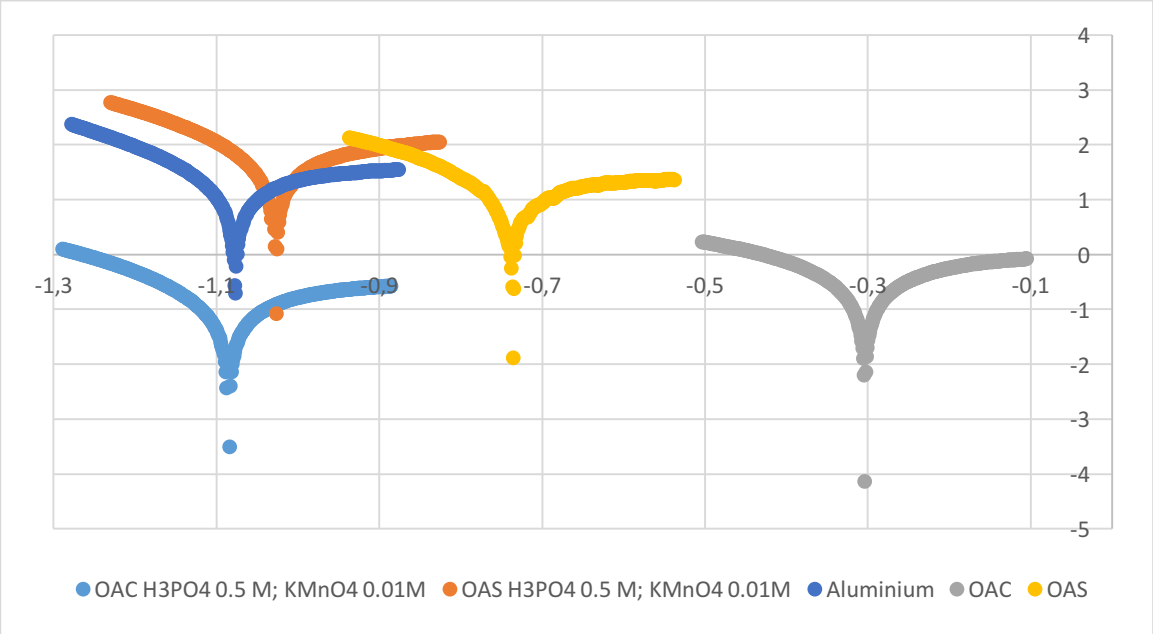

Graphic 14. Tafel curves corresponding to pieces of Aluminium, OAC and OAS, deanodized OAC and OAS with H_3PO_4 0.5M and $KMnO_4$ 0.01M.

As it can be observed, E_{corr} (underneath point of each Tafel curve) of both OAC (E_{corr} = -1.085V) and OAS (E_{corr} = -1.028V) deanodized alloys are very close to the pure aluminium value (E_{corr} = -1.078 V) and very far from the values corresponding to both anodized pieces without deanodizing process. This means that the deanodizing process has been effective and a stripping of the alloy has been successfully achieved. All the potentials are measured versus the reference electrode Ag/AgCl (KCl 1 M).

Besides, in the *table 13* of page 31, there are detailed the corrosion potential values of pieces OAC and OAS before doing the deanodizing treatment. There is an important difference between those values and the ones obtained with this experimental design which shows a clear stripping of both pieces.

In view of the results obtained between the piece corresponding to the second bath of this experimental design, a XPS analysis was performed with the purpose of determine de species present in both pieces and in order to conclude that deanodizing has taken place. From this analysis no traces of any species of Cr has been found.

In the following graphic, the peaks corresponding with the metallic aluminium (the peak in the right with lower binding energy) and the oxidised forms of aluminium are showed. A

comparison is made between the industrial and the alternative baths for each piece (OAC and OAS). As it can be observed, the peak of metallic aluminium is quite high. It is a signal that the metallic aluminium substrate has been reached, and the process has been successfully achieved. Peaks corresponding with a higher concentration of copper were found, which could be another signal of deanodizing.

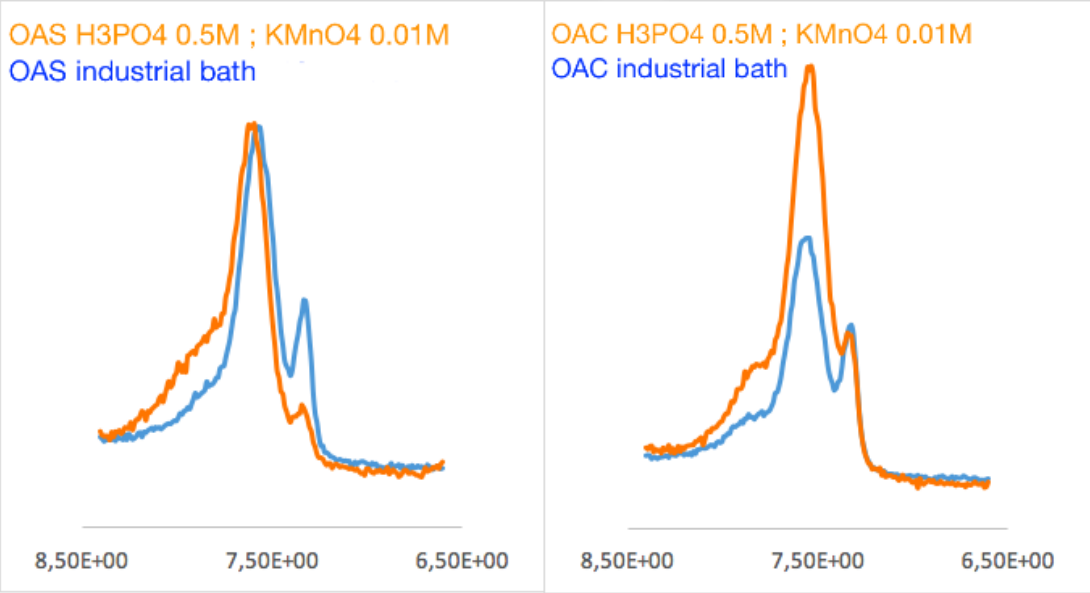

Graphic 15. XPS peaks corresponding to Al and Al_2O_3 or OAC and OAS after industrial deanodizing process and alternative deanodizing process.

4.5.5. Influence of potassium permanganate.

One last experimental design was developed with the purpose of evaluate the influence of changing the concentration of potassium permanganate in the deanodizing bath. Thus, four pieces were analysed with only two variable parameters: pH and [$KMnO_4$]. pH values have been increased up to 3 in two experiences and [$KMnO_4$] has been varying from 0.01 M up to 0.05 M. The experimental design conditions are detailed in the Annex 6.

In the case of this design, three pieces have been introduced in the baths during different times with the purpose of study the variation of the loss of thickness and the roughness with the time by analysing them with the chromatic confocal microscope. Nevertheless, only useful results were obtained for the firs experience of this design, experience which corresponds with

the number 2 of the fourth experimental design corresponding with the study of the influence of HF (H_3PO_4 0.5 M and $KMnO_4$ 0.01 M during 30 minutes). Pieces corresponding with the other baths were covered by a permanent black layer which was not removed with the application of an ultrasonic cleaning bath.

For the piece corresponding with the experiment 1 of this experimental design (a H_3PO_4 0.5 M and $KMnO_4$ 0.01 M), for both of them, the loss of thickness was measured for pieces after 10, 20 and 30 minutes with the purpose of study the loss of thickness with the time of deanodizing.

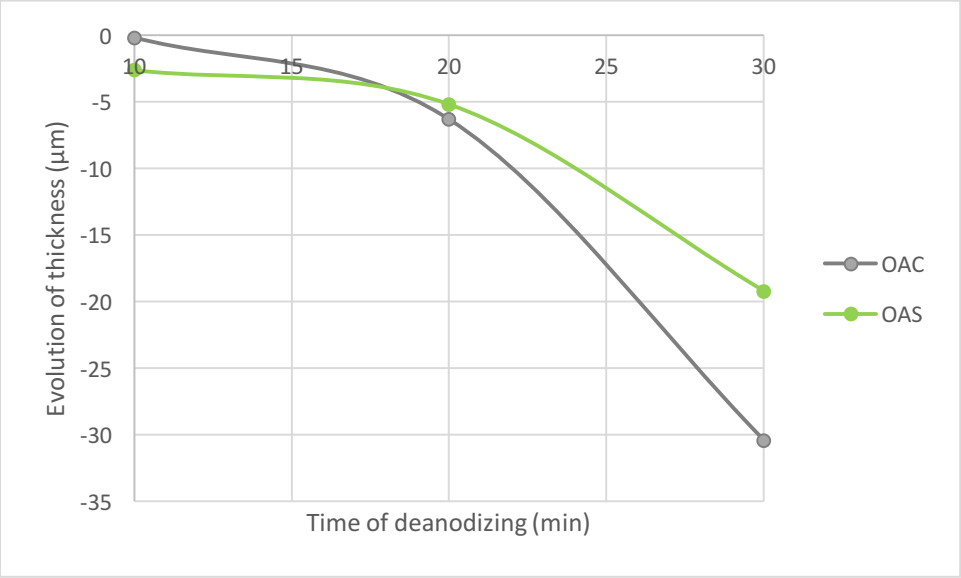

Graphic 16. Loss of thickness vs. time of pieces corresponding to a H_3PO_4 0.5 M and $KMnO_4$ 0.01 M bath.

As it can be observed, during the first 20 minutes for both type of pieces, the loss of thickness is not as intense as in the last 10 minutes. So, for a bath with this composition, the duration of the process would be the best by applying a time not greater than 20 minutes.

Actually, if results showed in *table 12* and *table 13* are compared with the results in this graphic, it can be observed that for 20 minutes of this bath treatment the same results are obtained with 30 minutes of the industrial deanodizing bath.

5. Conclusions.

After several analysis and the development of numerous deanodizing bath with different compositions and different acids employed through five experimental designs, some conclusions can be summarized from all the work which has been carried out.

- It has been concluded that the use of H_2SO_4 in the same concentration of H_3PO_4 does not allow an effective deanodizing of the pieces studied.
- The presence of HF in the deanodizing bath increases the attack over the piece but is not more effective over the deanodizing.
- The increasing of pH in the deanodizing bath decreases the degree of attack of the acids over the piece's surface, slowing down the deanodizing process. This fact confirms the role of H_3PO_4 as solvent of the Al_2O_3 anodized layer.
- The use of H_3PO_4 is essential in order to carry out an effective deanodizing over the pieces studied.
- The similarities between $KMnO_4$ and H_2CrO_4 in industrial deanodizing baths have been validated. Even the results with the employ a small concentration of $KMnO_4$ instead H_2CrO_4 in some cases are better. A high concentration of $KMnO_4$ is not effective. Concentrations near 0.01M have to be studied in order to get the best results.

Although a definitive bath composition has not been given yet, there is now a starting point from where design the optimum deanodizing bath. The role of each compound in the new deanodizing bath has been verified, and only an optimization of the final concentrations of each one in the bath and a XPS analysis of the last pieces have to be done.

6. References.

[1] Carriedo, G. A. *La química inorgánica en reacciones*, 1ª ed. (2010). Sintesis.

[2] Shakhashiri. Aluminum. *Chemical of the week*, (2008).

[3] *Al 2024, data sheet* (s.f.). Alcoa Global Rolled Products.

[4] Heber, K. V. Studies on porous Al2O3 growth. *Electrochimica Acta , 23* (1978), 127-133.

[5] J. S. Safrany. Anodisation de l'aluminium et de ses alliages. *Techniques de l'Ingenieur* (2008).

[6] *No. 71:10099–10385*, Federal Register, 2006, p. 71

[7] *Annexe XVII*. Service national d'assistance réglementaire REACH. Ministère de l'Environnement, de l'Energie et de la Mer.

[8] J. Lee, Y. Kim, H. Jang, W. Chung. Cr_2O_3 sealing of anodized aluminium alloy by heat treatment. *Surf. Coat. Technol*, 243 (2014), 34 – 38.

[9] Aluminium et alliages d'aluminium, NF EN 12373-2, *Norme Française*.

[10] ASTM B 680, *American society for testing and materials*.

[11] A. Mitsuhashi, K. Asami, A. Kawashima, K. Hashimoto; The corrosion behaviour of amorphous nickel base alloys in a hot concentrated phosphoric acid. *Corrosion Science*, Vol. 27 (1987) 957 – 970.

[12] I. Danilidis, J. Hunter, G.M. Scamans, J.M. Sykes. Effects of inorganic additions on the performance of manganese-based conversion treatments. *Corrosion Science*, 49 (2007), 1559 – 1569.

[13] G. Yoganandan, J.N. Balaraju, V.K. William Grips. The surface and electrochemical analysis of permanganate based conversion coating on alclad and unclad 2024 alloy. *Applied Surface Science*, 258 (2012), 8880 – 8888.

[14] J.-T- Qi, T. Hashimoto, J.R. Walton, X. Zhou, P. Skeldon, G.E. Thompson. Trivalent chromium conversion coating formation on aluminium. *Surface & Coatings Technology*, 280 (2015), 317 – 329.

[15] I-Wen Huang, Belinda L. Hurley, Fan Yang, Rudolph G. Buchheit. Dependence on temperature, pH, and Cl^- in the uniform corrosion of aluminum alloys 2024-T3, 6061-T6, and 7075-T6. *Electrochimica Acta*, 199 (2016) 242 – 253.

[16] Douglas A. Skoog, F.J. Holler, S.R. Crouch. *Principios de análisis instrumental* (6^{th} edition), section 10, Cenage Learning.

[17] T.Kim, S.H. Kim, D. Do, H. Yoo, D. Gweon. Chromatic confocal microscopy with a novel wavelength detection method using transmittance. *Optics Express,* 21 (2013), 6286 – 6294.

[18] *Confocal Chromatic: Optical principles*. Stil S.A.

[19] Z. Shi, M. Liu, A. Atrens. Measurement of the corrosion rate of magnesium alloys using Tafel extrapolation. *Corrosion Science*, 52 (2010), 579 – 588.

[20] J.M. Pingarron, P.S. Batanero. *Química electroanalítica*. Ed. Sintesis.

[21] X. Li, S. Deng, H. Fu. Sodium molybdate as a corrosion inhibitor for aluminium in H_3PO_4 solution. *Corrosion Science*, 53 (2011), 2748 – 2753.

[22] P. Kwolek, A. Kaminski, K. Dychton, M. Drajewicz, J. Sieniawski. The corrosion rate of aluminium in the orthophosphoric acid solutions in the presence of sodium molybdate. *Corrosion Science*, 106 (2016).

7. Annexes.

7.1. Annexe 1. Optimization of temperature conditions.

Table 19. Pieces under study during the optimization of temperature phase.

Piece	*[H_3PO_4]*	*[H_2CrO_4]*	*[H_2SO_4]*	*[$KMnO_4$]*	*Temperature*	*Time*	*Result*
OAC	0.5	0	0	0.2	25	30	No changes
OAC	0.5	0	0	0.2	25	30	No changes
OAC	0.5	0	0	0	25	30	No changes
OAC	1	0	0	0	25	30	No changes
OAC	1	0	1	0	25	30	No changes
OAC	0.49	0,23	0	0	25	30	No changes
OAC	0.49	0,23	0	0	60	95	No changes
OAS	0.49	0,23	0	0	80-85	10	Deanodized
OAC	0.49	0,23	0	0	80-85	30	Deanodized
OAS	0.5	0	0	0	25	30	No changes
OAS	0.5	0	0	0	80-85	5	Deanodized
OAC	0.5	0	0	0	80-85	20	Deanodized (black layer)
OAC	0	0	0.5	0	80-85	30	No changes
OAS	0	0	0.5	0	80-85	12	Deanodized
OAC	1	0	0	0	80-85	6.5	Deanodized (black layer)
OAS	1	0	0	0	80-85	1	Deanodized
OAC	0	0	1	.	80-85	30	No changes
OAS	0	0	1		80-85	7.5	Deanodized
OAC	1	0	1	0	80-85	6.5	Deanodized (black layer)
OAS	1	0	1	0	80-85	1.5	Deanodized
OAC	0.5	0	0.5	0	80-85	13	Deanodized (black layer)
OAS	0.5	0	0.5	0	80-85	2.5	Deanodized
OAC	0.2	0	0	0	80-85	13.5	Deanodized (black layer)
OAS	0.2	0	0	0	80-85	4	Deanodized
OAC	0	0	0.2	0	80-85	30	No changes
OAS	0	0	0.2	0	80-85	17.5	Deanodized
OAC	0.2	0	0	0.1	80-85	15	Brown layer

OAS	0.2	0	0	0.1	80-85	7	Brown layer
OAC	0	0	0.2	0.1	80-85	30	No changes
OAS	0	0	0.2	0.1	80-85	22	Deanodized (brown layer)
OAC	0.2	0	0	0.2	80-85	30	Brown layer
OAS	0.2	0	0	0.2	80-85	17	Brown layer
OAC	0	0	0.2	0.2	80-85	30	Brown layer
OAS	0	0	0.2	0.2	80-85	20	Deanodized (brown layer)

7.2. Annexe 2. First experimental design conditions.

Temperature: 80 – 85 °C.

Table 20. First experimental design conditions.

Nº Experience	*$[H_3PO_4]$ (mol/L)*	*pH*	*$[KMnO_4]$ (mol/L)*	*Duration (min) OAC/OAS*
1	0.2	1.28	0	10/5
2	0.5	1.02	0	10/5
3	0.2	2	0	10/5
4	0.5	2	0	10/5
5	0.2	1.31	0.01	10/5
6	0.5	1.06	0.01	10/5
7	0.2	2	0.01	10/5
8	0.5	2	0.01	10/5
9	0.2	1.28	0	20/10
10	0.5	1.02	0	20/10
11	0.2	2	0	20/10
12	0.5	2	0	20/10
13	0.2	1.31	0.01	20/10
14	0.5	1.06	0.01	20/10
15	0.2	2	0.01	20/10
16	0.5	2	0.01	20/10

7.3. Annexe 3. Second experimental design conditions.

Temperature: 80 – 85 °C.

Duration: 10 min.

Table 21. Second experimental design conditions.

Nº Experience	*[H_3PO_4] (mol/L)*	*pH*	*[$KMnO_4$] (mol/L)*	*[HF] (mol/L)*
1	0.2	1.28	0	0
2	0.5	1.02	0	0
3	0.2	2.00	0	0
4	0.5	2.00	0	0
5	0.2	1.31	0.01	0
6	0.5	1.06	0.01	0
7	0.2	2.00	0.01	0
8	0.5	2.00	0.01	0
9	0.2	1.45	0	0.2
10	0.5	1.30	0	0.2
11	0.2	2.10	0	0.2
12	0.5	2.00	0	0.2
13	0.2	1.48	0.01	0.2
14	0.5	1.36	0.01	0.2
15	0.2	2.00	0.01	0.2
16	0.5	2.12	0.01	0.2

7.4. Annexe 4. Third experimental design conditions.

Temperature: 80 – 85 °C.

Duration: 10 min.

Table 22. Third experimental design conditions.

Nº Experience	*[H_2SO_4] (mol/L)*	*pH*	*[$KMnO_4$] (mol/L)*
1	0.2	0.35	0.001
2	0.5	0.14	0.001
3	0.2	1.80	0.001
4	0.5	1.93	0.001
5	0.2	0.36	0.01
6	0.5	0.01	0.01
7	0.2	1.75	0.01
8	0.5	2.01	0.01

7.5. Annexe 5. Fourth experimental design conditions.

Temperature: 80 – 85 °C.

Duration: 30 min.

$KMnO_4$ 0.01 M.

Table 23. Fourth experimental design conditions.

Nº Experience	*[H_3PO_4]*	*[HF]*	*pH*
1	0.2	0	0.84
2	0.5	0	0.55
3	0.2	0.2	0.56
4	0.5	0.2	0.34
5	0.2	0	1.95
6	0.5	0	1.98
7	0.2	0.2	1.09
8	0.5	0.2	1.91

7.6. Annexe 6. Fifth experimental design conditions.

Temperature: 80 – 85 °C.

Duration: 30 min.

H_3PO_4 0.5 M.

Table 24. Fifth experimental design conditions.

Nº Experience	*[$KMnO_4$]*	*pH*
1	0.01	0.56
2	0.05	0.33
3	0.01	3.03
4	0.05	3.19